Nuclear Instruments and Methods in Physics Research B 268 (2010) 3167–3170

Contents lists available at ScienceDirect

Nuclear Instruments and Methods in Physics Research B

journal homepage: www.elsevier.com/locate/nimb

Ion irradiation effects on tungsten-oxide films and charge state effect on electronic erosion

N. Matsunami [a,*], M. Sataka [b], S. Okayasu [b], H. Kakiuchida [c]

[a] Energy Science Division, EcoTopia Science Institute, Nagoya University, Furo-cho, Chikusa-ku, Nagoya 464-8603, Japan
[b] Japan Atomic Energy Agency (JAEA), Tokai 509-5292, Japan
[c] National Institute of Advanced Industrial Science and Technology (AIST), Nagoya 463-8560, Japan

ARTICLE INFO

Article history:
Received 14 October 2009
Received in revised form 24 May 2010
Available online 4 June 2010

Keywords:
WO_3
Electronic excitation
Non-equilibrium charge incidence

ABSTRACT

We have studied electronic- and atomic-structure modifications of polycrystalline WO_3 films (bandgap of ~3 eV) by ion irradiation. WO_3 films were prepared by oxidation of W films on MgO substrates and of W sheets. We find disordering or amorphization, the lattice expansion of ~1.5% and bandgap increase of 0.2 eV after 90 MeV Ni ion irradiation at $\sim 3 \times 10^{12}$ cm^{-2}. A broad peak of optical absorption appears around 1.6 μm by ion irradiation. We also find that the erosion yield by high-energy ions with the equilibrium charge exceeds 10^4 and that the erosion yield under ion impact with non-equilibrium charge (90 MeV Ni^{+10}) is ~1/5 of that with the equilibrium charge (89 MeV Ni^{+19}). Effects of depth dependence of the ion mean charge on the erosion yields are discussed. The erosion yield by low-energy ions is also presented.

1. Introduction

Electronic and atomic-structure modifications of non-metallic oxides and nitrides by high- and low-energy ions have been studied by the authors, e.g., electronic sputtering aiming systematic investigation of atomic displacement induced by electronic excitations, comparison between p-type (Cu_2O) and n-type (ZnO) semiconductors etc. [1–5]. At present, experimental data is poor to argue the difference of ion irradiation effects on between p- and n-type semiconductors and more data is desired. Interestingly, ion-induced decomposition of Cu_3N films has been found [5], knowing that Cu_3N films thermally decompose at 250–470 °C [6]. Notice that both sputtering and decomposition mean erosion of materials. In spite of small bandgap of Cu_3N (~1.4 eV), the electronic decomposition yield (~10^3) of Cu_3N films by high-energy ions is far larger than the yield estimated from the suggested bandgap dependence [7]. Even for low energy (~100 keV) Ne ion impact, the decomposition yield of Cu_3N is larger than a typical sputtering yield based on the elastic collision cascade. It is of interest to study electronic sputtering of non-metals with a small bandgap to see whether the Cu_3N results is exceptional or not and also influence of the incident charge of high-energy-heavy ions on near surface phenomena such as electronic sputtering. Because in many cases, the incident charge of high-energy-heavy ions differs from the equilibrium charge, though the characteristic length for attaining the equilibrium charge is unknown except for a limited case [8].

In this study, we have investigated ion irradiation effects on WO_3 films. This material is chosen because of relatively small bandgap (2.6–2.9 eV [9,10]) and easier detection by ion beam analysis owing to heavy elements. We describe high-energy ion irradiation effects on atomic structure and the optical properties, which are the radiation effects throughout the film and anticipated to be insensitive to the incident charge. We also present the electronic sputtering, the effect of the incident charge on the electronic sputtering by high-energy ions and compare it with sputtering by low-energy ions.

2. Experimental

WO_3 films were prepared by oxidation of W sheets for 10 min at 550 °C [11] and W films on MgO substrates for 0.5–3 h at 500 °C in air. Here, W films were deposited on MgO by using RF-sputter deposition at room temperature with W target (99.95% purity) in Ar gas. Crystalline structure of the film is examined by X-ray-diffraction (XRD). The XRD intensity of the films on MgO is found to be much larger than that on W. Rutherford backscattering spectroscopy (RBS) of 1.8 MeV He^+ and H^+ were used to obtain the film thickness and composition. Normal incidence or glancing incidence (40° to the surface normal) with the scattering angle of 160° are employed for RBS. The film thickness is 0.4–0.8 μm for WO_3 on W and 0.06–0.5 μm for WO_3 on MgO, and the composition is close to stoichiometric (W:O = 1:3) with the accuracy of 10%. In RBS, the

---

* Corresponding author. Tel./fax: +81 52 789 5204.
E-mail address: n-matsunami@esi.nagoya-u.ac.jp (N. Matsunami).

0168-583X/$ - see front matter © 2010 Elsevier B.V. All rights reserved.
doi:10.1016/j.nimb.2010.05.080

stopping power [12] and the WO_3 film density of 1.87 × 10^{22} W cm^{-3} (7.2 gcm^{-3}) were employed. The enhancement factor of non-Rutherford cross section for 1.8 MeV H on O is determined to be 3.15, by utilizing TiO_2 single crystal. RBS of 1.8 MeV He and H show that the composition remains unchanged after irradiation with high- and low-energy ions. Optical absorption was measured by using a conventional spectrometer. According to atomic force microscopy, the grain size distributes 40–100 nm and the surface roughness in term of root mean square of the height is ~2 nm for unirradiated films, and no appreciable modification was observed after 90 MeV Ni at 3.7 × 10^{12} cm^{-2}.

Ion irradiations were performed at room temperature and at normal incidence (channeling effect is insignificant because the films are polycrystalline). High-energy-heavy ions (200 MeV $^{136}Xe^{+14}$, 100 MeV $^{136}Xe^{+11}$, 90 MeV $^{58}Ni^{+10}$ and 60 MeV $^{40}Ar^{+6}$) and low-energy ions (100 keV Ne^+ and N^+) were obtained from the Tandem accelerator at JAEA, Tokai and the 200 kV accelerator at Nagoya University, respectively.

3. Results and discussion

Ion-irradiation-induced modifications of atomic- and electronic-structures in terms of XRD and optical absorption using WO_3 films on MgO are described first. These are bulk properties and thus the incident charge of high-energy ions is less significant. Description is followed by the electronic sputtering by high-energy ions which depends on the incident charge of the high-energy ion.

3.1. Atomic structure

XRD patters are shown in Fig. 1(a). Diffraction peaks at ~23°, 33°, 47° and 48° are assigned to be WO_3. It is noticed that W (110) at ~40° was not observed; indicating all W on MgO is oxidized into WO_3 (the ratio of the thickness of WO_3 over that of W is obtained to be 3.54 and is close to the ratio of the W density in W over WO_3). From the most intensive peak of WO_3 at ~23°, this peak is concerned hereafter; the planar spacing for XRD was obtained to be 0.3867 nm (sample variation of 0.3%). This value is close to 0.3846 nm of the c-axis length of the orthorhombic structure or 0.3844 nm, half of the c-axis length of the monoclinic structure [13]. These are so close that the crystalline structure cannot be distinguished, orthorhombic or monoclinic. After 90 MeV Ni^{+10} ion irradiation at 3.5 × 10^{12} cm^{-2}, the XRD intensity decreases to one tenth of that of the unirradiated film (Fig. 1(b)). Quite a large expansion of lattice parameter by 90 MeV Ni ion (~1.6%) was observed. For low energy (100 keV) ion irradiation, thinner films of ~0.06 μm was employed so that the projected range (0.152 μm for 100 keV N and 0.118 μm for 100 keV Ne, see Table 1) is larger than the film thickness. The XRD intensity of such thinner films is very weak and diffraction peak at ~21.5°, tentatively assigned to be WO_3, frequently appears additionally to the main peak at 23°. Similarly, the lattice parameter expansion of 0.5% was observed for 100 keV N^+ ion irradiation at 2.6 × 10^{15} cm^{-2}. Low-energy ion irradiation on the XRD intensity shows more complicated behavior than that by high-energy ion.

3.2. Optical property

Fig. 2 shows optical absorption spectra of unirradiated and irradiated with 90 MeV Ni^{+10} at 1.4 × 10^{12} cm^{-2}. It is observed that the absorbance around 1.6 μm increases by the ion irradiation. The peak is very broad and differs from absorption due to OH stretching mode (3 μm), HOH bending (6 μm) [14,15], WO stretching (15 μm) [15] and WO_3 (12 μm) [16]. The increase of the optical absorption could be due to the same mechanism for sample with hydrogen inclusion, i.e., polaron (electron associated with phonon) transition from W^{5+} at a site to W^{6+} at a non-equivalent site [16]. X-ray photoelectron (XPS) is under way to investigate this point. Increase of the absorbance takes its maximum of ~0.14 at 10^{12} cm^{-2} for 90 MeV Ni ion irradiation. Coloration in the visible region is unclear, because of oscillations in the absorbance due to interference of directly transmitted photon beam and reflected beam from the film-to-substrate interface. The bandgap (E_g) is determined by using the relation for indirect transition: $(\text{absorbance}*E)^{1/2}$ is proportional to $(E-E_g)$, E being the photon energy (Fig. 2(c) inset). The bandgap increases by ion irradiation (Fig. 2(c)) and the bandgap

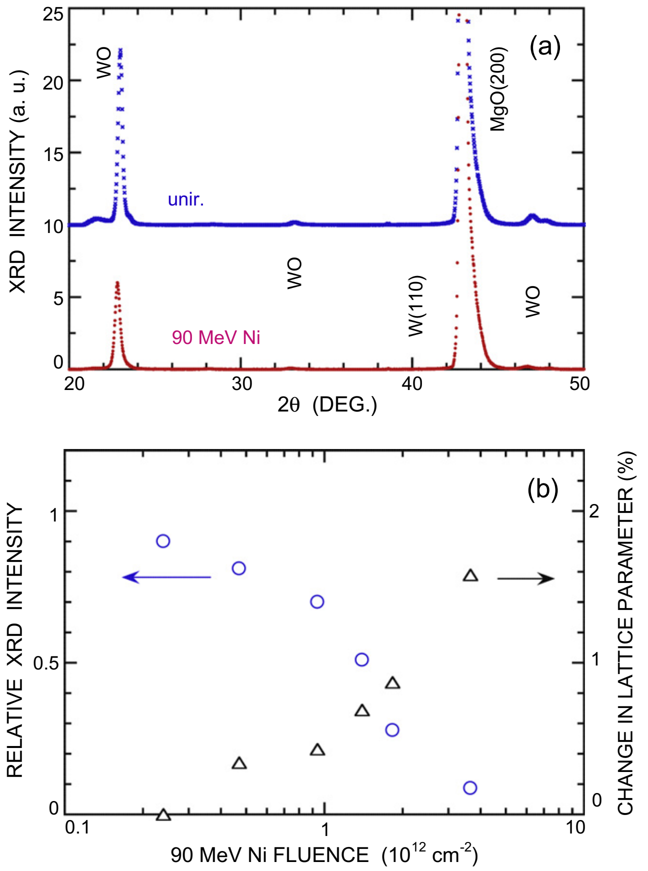

Fig. 1. (a) XRD patterns of unirradiated WO_3 film on MgO substrate (upper curve) and of a film irradiated with 90 MeV Ni at 1.4 × 10^{12} cm^{-2} (lower curve). Peaks at ~23°, 33°, 47° and 48° are assigned to be WO_3 and 42.9° MgO (2 0 0). W (1 1 0) at ~40 was not observed. For visible clarity, the intensity before irradiation is shifted by 5. Thickness of the film shown in this figure is ~0.43 μm. (b) Relative XRD intensity (O) and change in lattice parameter (Δ) vs 90 MeV Ni fluence. Estimated errors of XRD intensity and change in lattice parameter are ~20% and 0.3%, respectively.

Table 1
Equilibrium charge (Q_e), electronic (S_e), nuclear (S_n) stopping power (keV/nm), projected range (R_p) in WO_3 and sputtering yield Y of WO_3. The initial thickness used for 100 keV Ne and N ion irradiation is 56 and 59 nm, respectively. TRIM1997 [12] was used to calculate S_e, S_n and R_p.

Ions	Q_e	S_e (keV/nm)	S_n	R_p (μm)	Y
198 MeV Xe	30	24.5	0.1115	14.3	2.14 × 10^4
99 MeV Xe	25	19.03	0.194	9.91	1.14 × 10^4
89 MeV Ni	19	13.46	0.0299	9.74	2.34 × 10^3
60 MeV Ar	13	7.585	0.0133	9.84	326
100 keV Ne		0.243	0.19	0.118	11
100 keV N		0.305	0.0867	0.152	~4